Technical Report 32-1239

Effects of Alkali Metal Gettering Agents on Stainless Steel Corrosion

Wayne Phillips

APR 1968

RECEIVED
NASA STI FACILITY
INPUT BRANCH

JET PROPULSION LABORATORY
CALIFORNIA INSTITUTE OF TECHNOLOGY
PASADENA, CALIFORNIA

April 1, 1968

NATIONAL AERONAUTICS AND SPACE ADMINISTRATION

Technical Report 32-1239

Effects of Alkali Metal Gettering Agents on Stainless Steel Corrosion

Wayne Phillips

Approved by:

D. R. Bartz, Manager
Research and Advanced Concepts Section

JET PROPULSION LABORATORY
CALIFORNIA INSTITUTE OF TECHNOLOGY
PASADENA, CALIFORNIA

April 1, 1968

Page intentionally left blank

Foreword

A large amount of data on various alkali metals and their effect on containment materials is currently available in the literature. Almost all of this data is concerned with one alkali metal under a specific test condition. Among the data available are numerous references to the effects of various interstitial impurities on corrosion; in many instances, these effects are postulated on the basis of apparently anomalous data.

This work was undertaken in an attempt to further define the role of impurities in alkali metal corrosion and to determine whether gettering will minimize corrosion rates. In addition, several alkali metals were used to provide a quantitative evaluation of their relative corrosive effects on stainless steel.

Acknowledgment

Contents

Tables

Contents (contd)

Tables (contd)

Figures

Contents (contd)

Figures (contd)

Abstract

Stainless steel tilting capsules were used to study the effect of yttrium gettering in alkali metal corrosion flow streams of lithium, cesium, rubidium, and potassium. Tests carried out at 1500 and 1750°F indicated the feasibility of utilization of type 321 stainless steel for alkali metal containment up to the limit of structural capability, and the possibility of reducing the amount of corrosion and modifying the mode of corrosive attack by the use of flow stream gettering.

Effects of Alkali Metal Gettering Agents
on Stainless Steel Corrosion

I. Introduction

The need for accommodation of high-heat fluxes in space-power nuclear reactors has produced an interest in liquid metals as a working fluid. Among the properties desired in a nuclear reactor coolant have been low melting point coupled with a high boiling point, high specific heat, high thermal conductivity, low viscosity, and low density. These criteria have produced the current interest in lithium as a reactor coolant or primary working fluid (Ref. 1).

The Rankine cycle concept has led to the consideration of other alkali liquid metals for the boiling portion of the system. In this case, the desired radiation temperature, vapor pressure, and the effects of molecular weight on turbine design have been among the factors considered in a fluid selection. These factors have led to the consideration of potassium, cesium, or rubidium as a fluid (Refs. 2, 3, and 4).

A single-loop Rankine cycle concept has been under investigation at Oak Ridge National Laboratory (ORNL), using potassium as a fluid with in-core boiling. This system was envisioned to employ stainless steel for containment rather than refractory metals (Ref. 5).

The use of refractory metals for the primary coolant loop and stainless steel for the lower-temperature secondary loop has also been under consideration. A possibility also exists for using stainless steel containment of a two-loop system. This usage may be considered practical only in a small space-power reactor (100-kWe range) where radiator weight is a small portion of system weight and the weight penalty for a reduced radiation temperature might be acceptable.

In any of these system concepts, materials problems are of major concern. This concern is particularly true of the corrosion aspects of this problem. The work reported herein was undertaken to provide comparative data on the behavior of various alkali-liquid metals in stainless steels and to determine to what degree corrosion and mass transfer can be reduced by gettering agents in the alkali-liquid metal stream.

II. Literature Review of Test Materials Corrosion

A. Corrosion Mechanisms

Corrosion by a liquid-metal working fluid in a practical system results from the system being nonisothermal and containing more than one constructional material. A variety of complex corrosion processes can occur as the system attempts to attain equilibrium.

The type of corrosion observed in a test will depend not only on the type of test, materials, and working fluid selected, but also on test variables that are not always controllable. Among the corrosion mechanisms are:

(1) Simple dissolution of the containment material by the working fluid.

(2) Intergranular penetration.

(3) Impurity reactions.

(4) Temperature and/or concentration gradient mass transfer.

1. Material dissolution. The dissolution of the containment material by the working fluid is the simplest of the corrosion mechanisms. The extent of dissolution can be determined by isothermal tests. Prediction of the extent of this corrosion can be made if solubility information is available. R. L. McKisson and R. L. Eichelberger, in their review of existing solubility data (Ref. 6), concluded that reproducibility of data is difficult to attain. They attributed this difficulty in part to the interaction of impurities in the solvent with the solute.

A typical illustration of this problem is the data gathered by J. H. Swisher (Ref. 7) at the Lewis Research Center. His data for solubility of iron in liquid potassium at 1144°K displayed a variation of two orders of magnitude as the sampling cup metal was varied through the series: nickel, molybdenum, columbium, tantalum, and zirconium. The results were explained by assuming that the solubility of iron is a function of the oxygen concentration in the potassium, which in turn is controlled by the gettering action of the cup materials.

A general correlation was made in Ref. 7 between the observed iron solubility and the standard free energy of formation of the sampling cup metal oxides. The solubility of iron increased in a regular manner with decreasing free energy of formation of the sampling cup metal oxides. The use of standard free-energy data was considered valid because the surfaces of the cups were believed to be saturated during the course of the tests, and the principle of local equilibrium was believed to apply. Similarly, nitrogen has also been reported to increase the solubility of many metals in lithium (Ref. 8).

2. Intergranular penetration. Intergranular penetration has also been attributed to the action of impurities. In this case, the impurities are in the containment metal rather than in the working fluid. Typical of this type of attack is the penetration of oxygen-contaminated columbium by lithium (Ref. 9). Another example reported by E. E. Hoffman (Ref. 1) is the intergranular penetration by lithium of iron containing carbon.

3. Mass transfer. Temperature-gradient mass transfer and concentration-gradient mass transfer may not be observed in a static isothermal test. These transfers may be detected only after a flow system has been operated for an extended period of time.
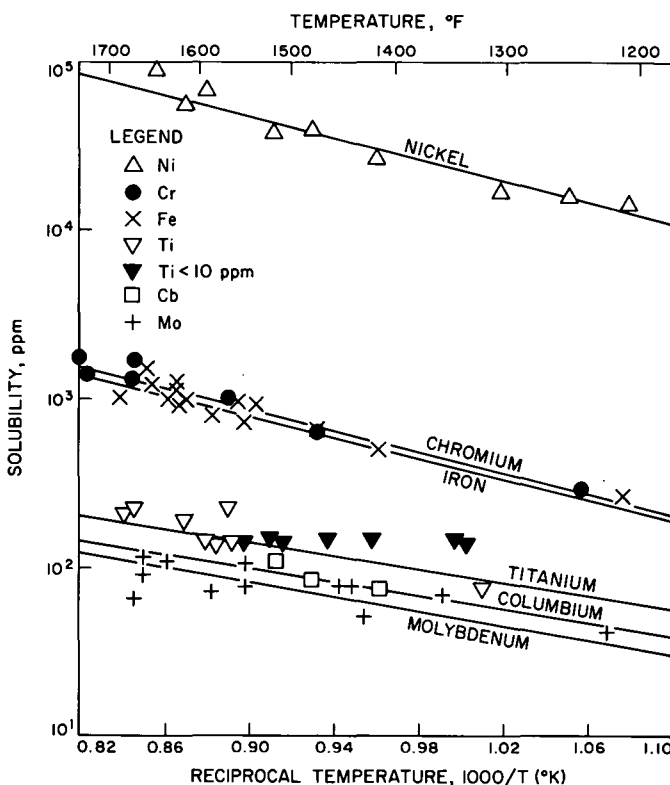

Fig. 1. Solubility of some metals in lithium (data from Ref. 10)

Temperature-gradient mass transfer can be studied in a thermal-convection loop, or in a tilting capsule where a temperature gradient is maintained along the length of the capsule and a liquid metal flow is obtained by a periodic inversion of the capsule. The driving force for corrosion in this case is the variation of solubility of the container material in the liquid metal as a function of temperature. The variation of solubility of some metals in lithium and potassium as a function of temperature was reported in Refs. 6, 7, 10, 11, and 12, from which Figs. 1 and 2 were compiled. Dissolution of the container material takes place at the hot end of the capsule and reprecipitation occurs at the cold end. This mechanism, in some cases, can be sufficiently extensive to cause system plugging.

a. Lithium circulation loops. Both pumped and thermal circulation loops have been run with some combinations of liquid metals and containment materials. From

LEGEND
O, △ Mo COLLECTOR; ~20 ppm O_2 IN K
▲,■ Cb COLLECTOR; ~20 ppm O_2 IN K
X Fe SOLUBILITY; W COLLECTOR; 8-10 ppm O_2 IN K
+ Ni SOLUBILITY; W COLLECTOR; 8-10 ppm O_2 IN K
⊗ Fe SOLUBILITY; W COLLECTOR; 16 ppm O_2 IN K

Fig. 2. Solubility of iron, nickel, and cobalt in potassium (data from Refs. 6, 7, 11, and 12)

the results obtained with lithium in forced circulation loops, Pratt and Whitney Aircraft (Canel) concluded that stainless steels are unsuitable for use in the 1300–1500°F temperature range with lithium (Ref. 8). Their data indicate that some change in type of corrosion, or in corrosion rate, can be obtained by the addition of a gettering agent in the containment material (type 321 or 347 stainless steel). They also found that an addition of a titanium gettering agent in the lithium flow stream eliminated intergranular corrosion in pure iron test loops.

Work by J. H. Swisher at the Lewis Research Center (Ref. 7) on the solubility of iron, nickel, and cobalt in potassium led him to conclude:

(1) Iron-rich alloys are limited as containment materials and are dependent upon the control of the oxygen level in the liquid potassium.

(2) Nickel and cobalt are not limited in liquid potassium by the solubility criteria.

b. Potassium convection loops. Potassium thermal convection loops of type 316 stainless steel, run at ORNL (Ref. 2) in the 1500–1600°F range showed consistent weight losses in the hot zone and weight gains in the cold zone. These effects were relatively slight (equivalent of a wall thickness reduction of 0.06 mil) during the 3000-h test.

The deposits showed some preferential leaching of chromium and nickel. A significant movement of carbon was detected, however. Carbon content of the subcooler surfaces (1250°F) increased to 0.5 wt %, which resulted in a post-test elongation at fracture of 15.5% of a tensile specimen located in this area. This result compares with 51.5% for control specimens. Specimens from other portions of the loop showed significant drops in yield strength, but only slight changes in elongation and ultimate tensile strength.

B. Role of Interstitials

These data indicate that interstitial type impurities play a significant role in the corrosion phenomena encountered during potassium containment by ferrous base alloys.

The aggressiveness of cesium and rubidium does not appear to be as great as that of potassium; however, limited test information is available on cesium. This test information (Refs. 13–15) indicates no attack by cesium
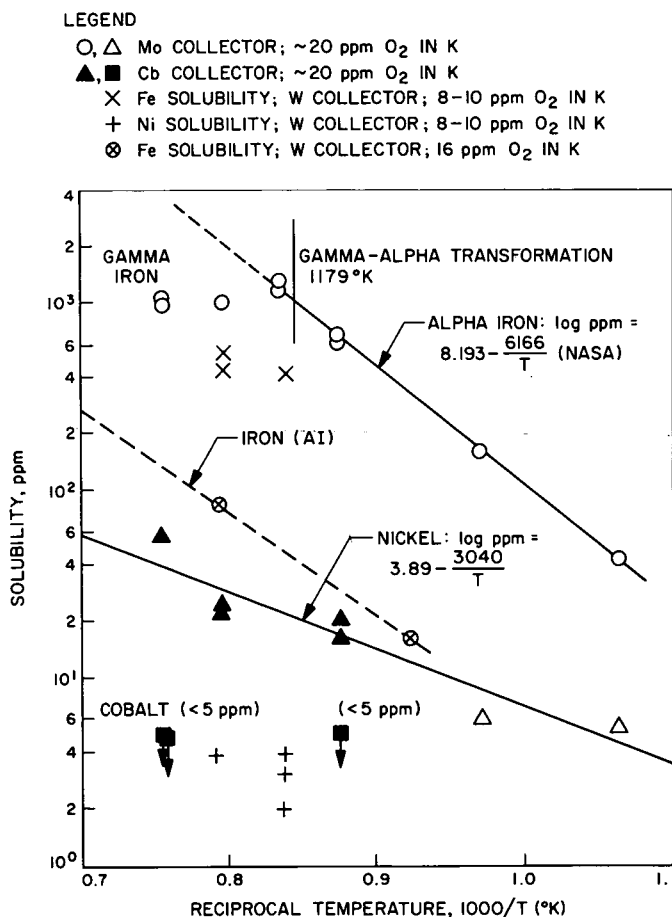
on iron or on 17-4PH, AM-350, type 416, and type 304 stainless steels. Despite the reduced activity of cesium, a slight carbon transfer problem was observed with type 310 stainless steel in these tests.

Work done at Mine Safety Appliances (MSA) Research Corp. indicated low solubilities of the constituents of Haynes-25 (L605) in cesium (Ref. 16) and their results are listed in Table 1. Dissimilar metal mass transfer was observed in couples of L605 vs Cb-1Zr. Interstitial element transfer from the L605 to Cb-1Zr was prevalent and the observation was made that one nonmetallic transfer apparently affects the transfer rate of other nonmetallics.

The role of interstitials in increasing the corrosiveness of cesium was shown by work done at the Rocketdyne Div. of North American Aviation and MSA Research Corp. The workers at Rocketdyne (Ref. 14) found that attack of a molybdenum reflux capsule was greater in the 2500°F liquid region than the attack found in the 1800°F condensing region of a second capsule of identical design. The 1800°F condensing region was exposed to high purity condensed vapor that is normally considered to be much more corrosive than a liquid saturated with metallic impurities. There is some question as to whether this anomalous corrosion rate was caused by contamination of the cesium or by splashing of the cesium in the pool boiling regime used in the test. Splashing would allow precipitation of dissolved molybdenum from the cesium onto the cooler condensing upper area of the reflux capsule. This precipitation

would then be followed by dissolution of the molybdenum in the hotter liquid area until saturation of the cesium was again attained.

Identical tests using Cb-1Zr capsules produced greater attack at 1800°F than at 2500°F. These results can almost certainly be attributed to contamination or impurities.

Similar tests run at MSA Research Corp. with zirconium tabs present in a Mo-0.5 Ti reflux capsule showed very little corrosion and no mass transfer after cesium exposure at 2500°F for 725 h (Ref. 17). Thus, it is believed that the gettering of interstitials by the zirconium almost eliminated corrosion of the molybdenum container by the cesium.

Corrosion of L605 in rubidium was investigated at Aerojet-General (Ref. 18). Although they concluded that L605 was not corroded by rubidium at 1400 or 1700°F in 1000 h, anomalous hardness and property changes were observed. Anomalies were also observed in solubility data. Although a study of the data did not reveal any correlations between high oxygen content and increased concentrations of oxygen, the possibility of this effect cannot be disregarded without performing more specific and precise experiments.

The role of impurities in the corrosion has been tentatively identified as the formation of complexes with the impurity, the liquid metal, and the containment metal. Some of these complexes have been identified (Refs. 19–22), among them are $KCbO_3$ and $(Na_2O)_2 \cdot FeO$.

Some attempts have been made to evaluate the effectiveness of gettering agents in a containment alloy for reducing interstitial element transfer. Work (Ref. 23) by Goldmann, et al., with potassium thermal convection loops, which were constructed of type 316 stainless steel and operated between 1200 and 1600°F, indicated the transfer of carbon from the hot to the cold portions of the loop. Insertion of type 321 stainless steel tabs in the loop of type 316 stainless steel resulted in carbon pickup by the type 321 sample in the cold leg, but no loss of carbon by the sample in the hot leg. Since the type 316 stainless steel loop provided a large source of unstabilized carbon, no conclusion could be drawn with regard to the behavior of an all type 321 stainless steel loop. Weight changes of the type 321 stainless steel tabs were found to be equivalent to those found with type 316 stainless steel.

Table 1. Content of Haynes-25 components in cesium at 1800°F[a]

Item	Tests		
	HS1	HS2	HS3
Exposure, h	10	100	1000
Co, ppm	125	<6	12
Ni, ppm	18	<6	<6
Fe, ppm	9	<6	<1
Cr, ppm	18	<6	<6
W, ppm	—	—	<12
Al, ppm	156	<6	1200
[a]Reprinted from Ref. 16 by permission of MSA Research Corp.			

R. W. Harrison (Ref. 24) found that carbon and nitrogen transfer from 316 stainless steel to Cb-1Zr alloy in a potassium atmosphere was eliminated by the use of type 321 stainless steel that was stabilized with an addition of titanium.

III. Tilting Capsule Tests

A. Selected Test Materials

To further characterize the role of impurities in alkali liquid metal corrosion, a series of tilting capsule configurations was selected for test. Stainless steel was selected for a containment material on the basis that some data are available, iron compounds play a role in the corrosion process, and a wide variety of commercial alloys are available. It was decided to use a stainless steel that was stabilized, or contained an alloy addition that formed a stable compound with interstitials. Type 321 stainless steel, a titanium stabilized alloy, was selected for this purpose. To provide a contrasting alloy, type 410 stainless steel, a straight chromium type alloy, was selected. The analyses of both stainless steel materials are given in Table 2.

Testing was done both with and without a gettering agent in the liquid metal stream. Yttrium was selected for this gettering agent on the basis of the stability of its oxides and nitrides as compared to the stability of the oxides (Ref. 25) and nitrides (Ref. 26) of the alkali liquid metals (Tables 3 and 4). To check the mass transfer rate of yttrium, a capsule was run with the yttrium in the hot end and another was run with the yttrium in the cold end.

The alkali liquid metals selected for test were those of interest or possible interest in Rankine-cycle space-power systems, namely lithium, potassium, cesium, and rubidium. The lithium used in this experiment was Nuclear Grade supplied by Foote Mineral Company.

Table 2. Analyses of stainless steels before test

Element	Type 321[a]		Type 410[a]	
	Tube	Sheet	Tube	Sheet
Al	<0.01	<0.01	<0.01	<0.01
Cb	<0.01	<0.01	<0.01	<0.01
Co	0.13	0.14	<0.005	<0.005
Cu	0.10	0.22	0.08	0.09
Cr	18.30	17.35	12.00	12.00
Mn	1.53	1.62	0.43	0.29
Mo	0.20	0.32	<0.15	0.20
Ni	11.50	11.20	0.21	0.31
Pb	<0.01	<0.01	<0.01	<0.01
Si	0.70	0.72	0.55	0.48
Sn	<0.003	<0.003	<0.003	<0.003
Ta	<0.01	<0.01	<0.01	<0.01
Ti	0.47	0.47	0.08	0.09
V	0.05	0.04	<0.01	<0.01
W	<0.01	<0.01	<0.01	<0.01
C	0.09	0.08	0.10	0.12
H	2ppm	1ppm	2ppm	5ppm
N	0.012	0.010	0.030	0.030
O	0.008	0.006	0.004	0.012
P	0.016	0.018	0.017	0.018
S	0.009	0.005	0.012	0.010

[a] In % unless noted otherwise.

Table 3. Free energies of formation of oxides[a]

Compound	900°K[b]	1200°K[b]
Li_2O	−114	−97
Na_2O	−69	−55
K_2O	−54	−42
Rb_2O	−49	−31
Cs_2O	−42	−24
NiO	−37	−33
CoO	−41	−35
FeO	−49	−45
$\frac{1}{3}Cr_2O_3$	−72	−69
Vo	−81	−76
$\frac{1}{2}TiO_2$	−88	−82
$\frac{1}{3}Y_2O_3$	−120	−114
$\frac{1}{2}ZrO_2$	−110	−104

[a] Reprinted from Ref. 25 by permission of authors.

[b] In kcal/g-atom of O.

Table 4. Free energies of formation of nitrides[a]

Compound	ΔF_{298}[b]	ΔH_{298}[b]	ΔS_{298}	Melting point, °K
Li_3N	−37.3	−47.5	−34.2	d[c] 548
Rb_3N	−	−	−	594
K_3N	−	−15.0 to −20.0	−	616
Cs_3N	−	−	−	599
YN	−64.0	−71.5	−25.0	−
1/4 Si_3N_4	−38.7	−44.8	−20.4	subl[c] 2170
VN	−34.5	−40.8	−21.0	2320
Cr_2N	−	−26.3	−	−
CrN	−	−28.3	−	d 1770
Mn_4N	−	−39.9	−	−
Fe_4N	+0.89	−2.6	−11.5	met[c]
1/5 P_3N_5	−	−15.0	−	−
Cu_3N	−	+17.8	−	met

a Reprinted from Ref. 26 by permission of McGraw-Hill Book Co., Inc.
b In kcal/g-atom of N.
c d = decomposes; subl = sublimes; met = metastable.

Table 5. Typical analyses of lithium, cesium, rubidium, and potassium metals

Element	Li[a]	Cs[a]	Rb[a]	K[a]
Fe	30	<5	<5	20
B	~100	<5	<5	<10
Co	<5	<5	<5	<5
Cd	−	−	−	25
Mn	1	<1	<1	3
Al	20	25	5	5
Mg	35	<1	<2	5
Sn	<5	<5	<5	<5
Cu	3	<5	<2	10
Pb	<5	<10	<5	<5
Cr	2	<5	<5	<5
Si	>0.1%	<25	<10	<25
Ti	<5	<5	<5	<5
Ni	~400	<5	<5	5
Mo	<5	<5	<5	<3
V	<5	<5	<5	<1
Be	<1	<1	<1	<1
Ag	<1	<1	2	<1
Zr	<10	−	−	<10

a In ppm unless noted otherwise.

The potassium, cesium, and rubidium were high purity types supplied by MSA Research Corp. Typical analyses of these materials are given in Table 5.

B. Test Description

To achieve good purity, the following materials and procedures were used in the tilting capsule tests:

(1) A furnace as shown in Fig. 3.

(2) Mullite tubes for containment of the inert atmosphere.

(3) High purity argon.

(4) Impurity levels in both the entrance and exit gas were monitored throughout the tests.

(5) A liquid argon supply to provide a gas moisture level of 1–2 ppm and an oxygen level of 2–3 ppm.

(6) Each capsule was protected from trace impurities in the cover gas during the test by a wrap of tantalum foil, since outgassing of the capsule and mullite tube usually required approximately 24 h at 500°F before the gas moisture and oxygen levels were reached.

(7) Cycling was done at the rate of 1 cycle/min with a 45-deg tilt in each direction.

Testing was done at two hot-end temperatures, 1500 and 1750°F. In both cases, a 300°F temperature differential was maintained along the length of the capsule during the 500-h test.

The components of the test capsules are shown in Fig. 4. A single length of tubing of each material was used for fabrication of all the test capsules of one type. Likewise, test tabs, end caps, and weld rings were fabricated from a single sheet of material. Analyses of these materials are given in Table 2.

Test tabs were milled to a uniform size and deburred. The test materials were degreased in trichloroethylene and pickled in a solution of sulphuric and hydrofluoric acids diluted in water. A distilled water rinse was followed by air drying.
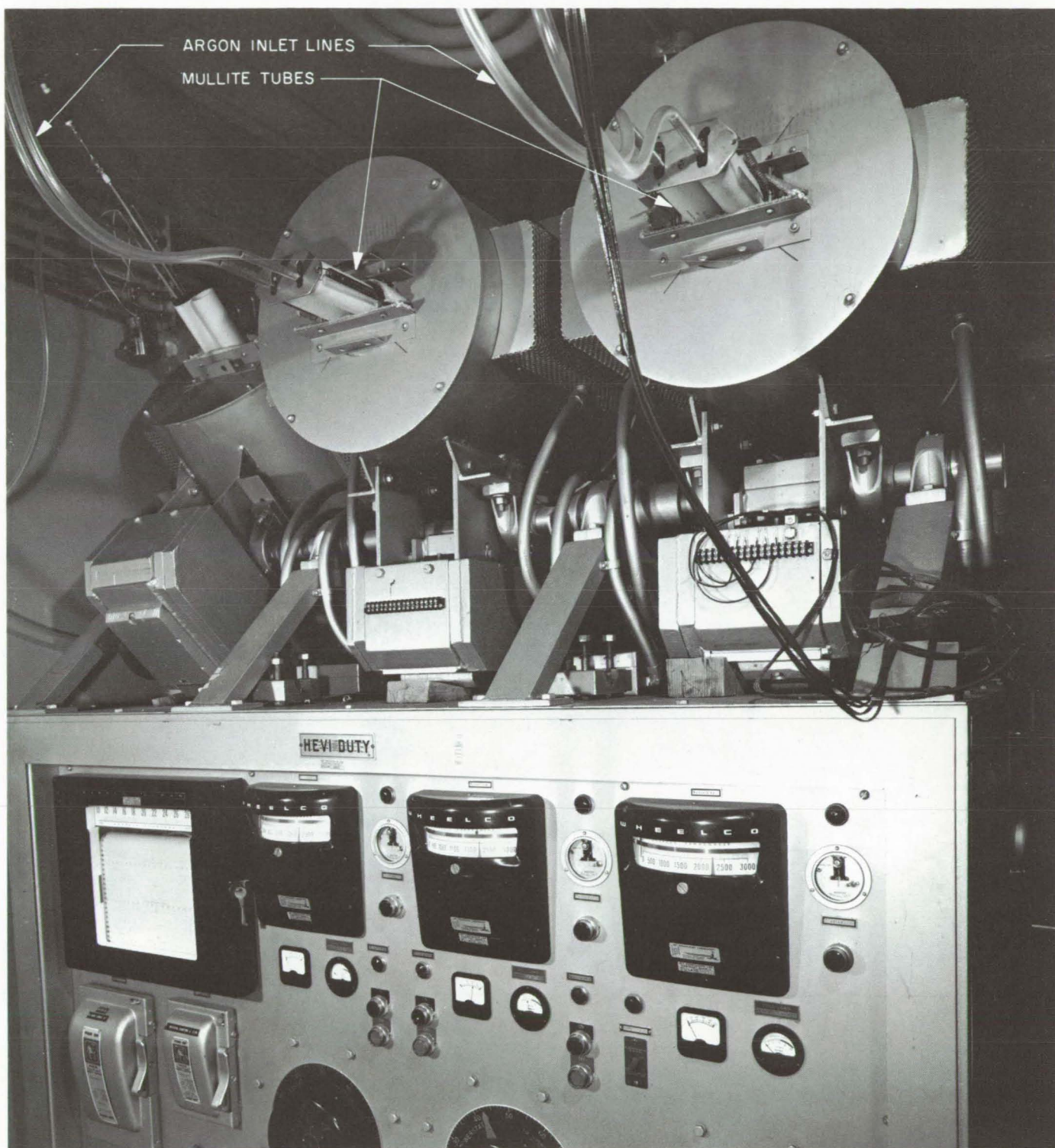
Fig. 3. Tilting furnace test installation
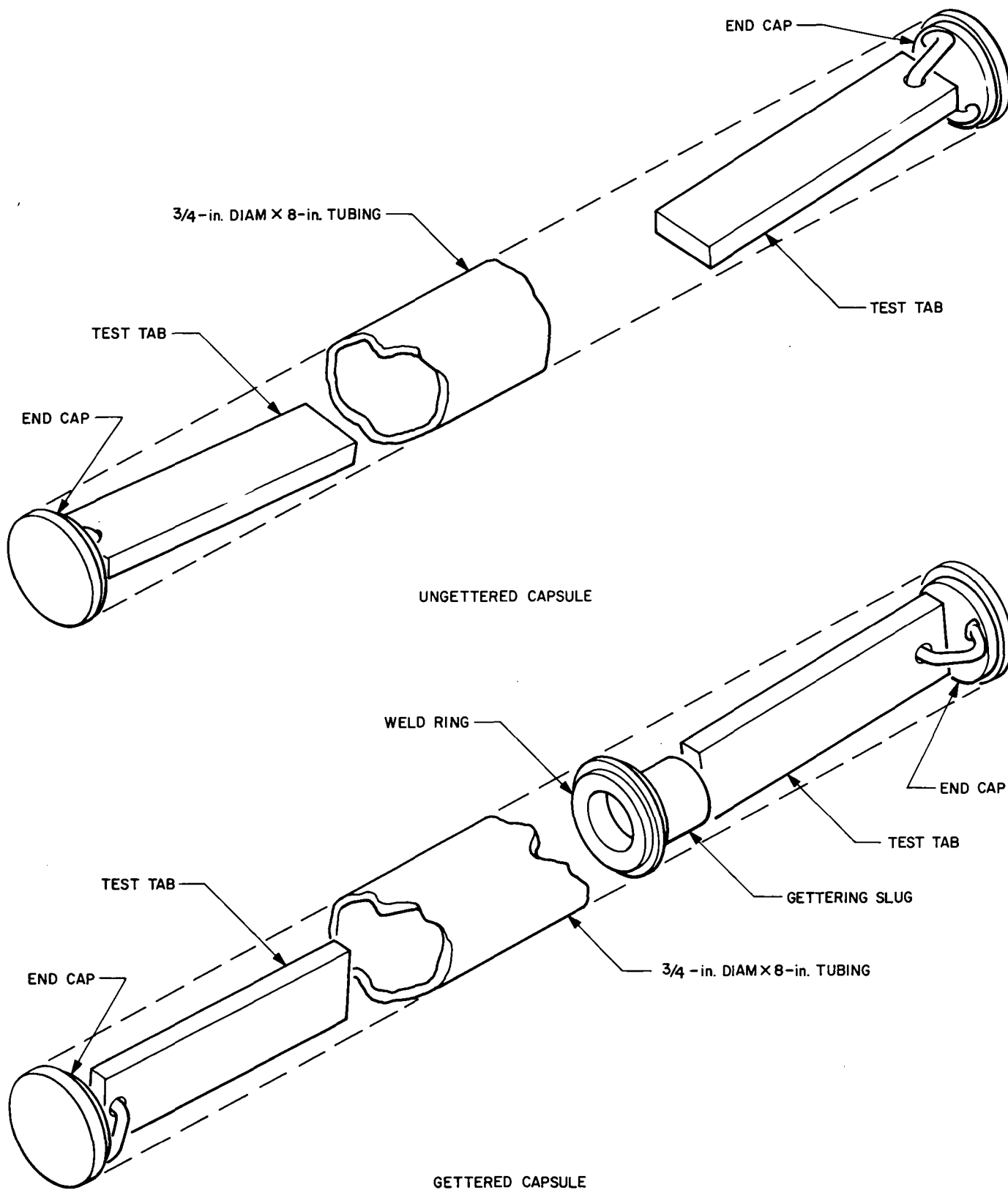
END CAP

3/4-in. DIAM × 8-in. TUBING

TEST TAB

TEST TAB

END CAP

UNGETTERED CAPSULE

WELD RING

END CAP

TEST TAB

GETTERING SLUG

TEST TAB

END CAP

3/4 -in. DIAM × 8-in. TUBING

GETTERED CAPSULE

Fig. 4. Tilting capsule test components

The lithium was received in the form of 1-lb blocks packed under helium in tin-plated cans. These blocks were melted into a stainless steel beaker and allowed to dross until solidification started to occur. The lithium was then cast into sticks, using a bottom pouring technique. The other liquid metals were received in 50-cm³ ampules. These liquid metals did not dross when they were melted. The capsules were filled by transferring 15 cm³ of molten metal from the ampule with a heated syringe.

Liquid metal handling and TIG (tungsten inert gas) welding of the capsules were done in a glove box, using a high-purity argon atmosphere. Liquid argon was used for the gas supply. Monitoring of the glove-box atmosphere was done with a Consolidated Electrodynamics Corp. moisture analyzer, and oxygen content was monitored with an Analytical Systems analyzer. Combined oxygen and moisture content was maintained below 5 ppm.

After test, the alkali metals were removed by reaction. Water was used to react the lithium capsules. A 50–50 mixture of kerosene and isopropyl alcohol was used for the other metals.

Test tabs were then removed, weighed, and measured for dimensional change. They were then machined into tensile specimens and tested. Part of the ruptured tensile specimens was submitted for chemical analysis. Sections of each end of the capsule and tensile specimens were used for metallography and microprobe analyses.

C. Test Results

1. Weight change data. The weight change data for type 321 stainless steel test capsules from the 500-h test, Table 6, indicate the following:

(1) Weight changes at 1500°F with cesium, rubidium, and potassium represent a thickness change of less than 0.02 mil; yttrium gettering had no effect on these results.

(2) Lithium produced an order of magnitude more weight change than the other three alkali metals at 1500°F.

(3) Lithium produced dissimilar metal mass transfer between the yttrium and the type 321 stainless steel at 1500°F, resulting in complete dissolution of the yttrium.

(4) Dissimilar metal mass transfer between the type 321 stainless steel and yttrium occurred at 1750°F with all four alkali liquid metals.

(5) Weight changes in the ungettered capsules of cesium, rubidium, and potassium increased negligibly as a result of the test temperature increase from 1500 to 1750°F.

(6) The 1750°F test with lithium resulted in weight loss in both test tabs; the loss is believed to be an indication of the lack of lithium circulation, rather than a valid effect.

Weight change data for type 410 stainless steel test capsules are presented in Table 7. These data indicate:

(1) All four alkali metals produced weight loss in both the hot and cold test tabs at both test temperatures, indicating solution corrosion to be the predominating mechanism under these test conditions, rather than mass transfer.

(2) The increase in test temperature from 1500 to 1750°F increased test tab weight losses by an order of magnitude for all but potassium capsules which displayed a decrease in corrosive attack. This anomaly in the potassium capsule data at 1750°F is considered to be due to a lack of flow, rather than a valid corrosion rate.

(3) Slight weight gains of the yttrium getter slugs were observed with cesium and rubidium at 1500°F. Lithium and potassium produced dissolution at this temperature.

A comparison of the weight change data for the two stainless steels indicate that cesium, rubidium, and potassium produced an order of magnitude more corrosion in the type 410 than in the type 321 stainless steel at 1500°F. This corrosion rate increased with temperature with the type 410 stainless steel, but displayed little change with temperature with the type 321 stainless steel.

Dissimilar metal mass transfer between yttrium and the type 321 stainless steel became rampant at 1750°F with all four alkali metals. With the type 410 stainless steel, dissolution of the yttrium became extensive at 1750°F, particularly with cesium and rubidium, but the effects were not catastrophic.

Table 6. Weight change test results, type 321 stainless steel[a]

Liquid metal	Y location	Test at °F	Weight changes, g[b]		
			Hot tab	Cold tab	Yttrium
Li	None	1500	−0.060	+0.038	—
		1750	−0.006	−0.077	—
Li	Hot end	1500	−0.213	+0.027	∞[c]
		1750	−0.216	−0.217	∞
Li	Cold end	1500	−0.065	−0.163	∞
		1750	+0.020	−0.591	∞
Cs	None	1500	−0.001	−0.007	—
		1750	−0.004	−0.006	—
Cs	Hot end	1500	−0.003	−0.001	+0.010
		1750	Rt[d]	Rt	Rt
Cs	Cold end	1500	−0.003	−0.001	+0.013
		1750	Rt	Rt	Rt
Rb	None	1500	−0.003	+0.001	—
		1750	−0.004	−0.004	—
Rb	Hot end	1500	−0.057[e]	−0.001	+0.018
		1750	Rt	Rt	Rt
Rb	Cold end	1500	−0.001	−0.001	+0.030
		1750	Rt	Rt	Rt
K	None	1500	−0.003	+0.001	—
		1750	−0.007	+0.005	—
K	Hot end	1500	−0.002	−0.001	+0.021
		1750	Rt	Rt	Rt
K	Cold end	1500	−0.006	+0.005	+0.002
		1750	Rt	Rt	Rt

[a]Nominal areas: test tab = 2¼ in.², yttrium slug = ¾ in.², total internal test capsule = 20 in.²; nominal volumes: test capsule = 2½ in.³, liquid metal = 1 in.³

[b]Accuracy of weighing estimated at ±0.001 g.

[c]Slug completely dissolved and redeposited on capsule walls.

[d]Rt = ruptured in test.

[e]Reaction area at tab-yttrium contact point.

Table 7. Weight change test results, type 410 stainless steel[a]

Liquid metal	Y location	Test at °F	Weight changes, g[b]		
			Hot tab	Cold tab	Yttrium
Li	None	1500	−0.038	−0.030	—
		1750	−0.502	−0.608	—
Li	Hot end	1500	−0.096	−0.059	−0.030
		1750	−0.001	−0.412	−0.060
Li	Cold end	1500	−0.043	−0.105	−0.017
		1750	−0.617	−0.558	−0.100
Cs	None	1500	−0.028	−0.045	—
		1750	−0.408	−0.301	—
Cs	Hot end	1500	−0.044	−0.081	+0.010
		1750	−0.413	−0.393	−0.527
Cs	Cold end	1500	−0.044	−0.015	+0.038
		1750	−0.534	−0.495	−0.067
Rb	None	1500	−0.032	−0.049	—
		1750	−0.436	−0.459	—
Rb	Hot end	1500	−0.031	−0.044	+0.017
		1750	−0.422	−0.337	−0.215
Rb	Cold end	1500	−0.042	−0.032	+0.018
		1750	−0.433	−0.429	−0.202
K	None	1500	−0.035	−0.032	—
		1750	−0.013	−0.344	—
K	Hot end	1500	−0.041	−0.033	−0.011
		1750	−0.024	−0.016	−0.028
K	Cold end	1500	−0.007	−0.031	+0.001
		1750	−0.014	−0.018	−0.003

[a]Nominal areas: test tab = 2¼ in.², yttrium slug = ¾ in.², total internal test capsule = 20 in.²; nominal volumes: test capsule 2½ in.³, liquid metal = 1 in.³

[b]Accuracy of weighing estimated at ±0.001 g.

2. Tensile data. Exposure to cesium, rubidium, or potassium at both test temperatures produced no change in room-temperature tensile properties of type 321 stainless steel (Table 8). Two of the tensile specimens exposed to lithium showed slightly decreased strengths, however the amount of decrease does not rule out data scatter as opposed to a true effect.

Scatter is also present in the data for type 410 stainless steel (Table 9). This scatter is a function of the amount of martensite present in the steel which in turn is a function of capsule cooling rate and maximum temperature.

Where test temperatures and cooling rates were sufficient to produce transformation to martensite, strength was greatly increased and ductility reduced. None of the tensile data for the type 410 stainless steel displayed any clear cut effects from alkali metal exposure.

3. Metallographic data. Visual and metallographic examination of the type 321 stainless steel capsules, tested at 1500°F, indicated negligible corrosive attack or mass transfer in any portion of the gettered or ungettered capsules containing cesium, rubidium, or potassium. The photomicrograph of Fig. 5 is typical for these capsules.

Corrosive attack was produced by lithium at this temperature (1500°F), however. Figure 6 shows the preferential grain boundary attack in the hot end of the ungettered lithium capsule.

Table 8. Room temperature tensile test results, type 321 stainless steel

| Liquid metal | Y location | Test at °F | Room temperature properties | | | | | |
| | | | Tensile strength | | Yield strength | | Elongation, % | |
			Hot tab	Cold tab	Hot tab	Cold tab	Hot tab	Cold tab
Li	None	1500	68,300	79,700	31,000	40,600	—	—
		1750	85,100	80,900	36,600	36,800	61	61
Li	Hot end	1500	77,200	76,300	36,400	39,500	—	65
		1750	71,000	82,000	33,000	40,600	—	65
Li	Cold end	1500	84,900	82,800	44,600	39,500	67	65
		1750	82,500	77,800	37,900	38,400	—	—
Cs	None	1500	88,000	81,200	40,400	40,200	68	—
		1750	86,400	87,500	31,700	28,800	56	57
Cs	Hot end	1500	87,500	80,500	42,500	43,200	67	67
		1750	83,700	85,200	34,200	33,500	55	55
Cs	Cold end	1500	80,100	83,300	36,400	44,000	—	—
		1750	87,300	85,100	30,400	29,800	55	55
Rb	None	1500	79,400	88,200	43,400	46,400	—	—
		1750	81,400	82,900	34,800	33,200	65	62
Rb	Hot end	1500	88,300	80,600	28,800	37,900	69	62
		1750	85,000	87,400	29,200	29,500	56	56
Rb	Cold end	1500	84,800	78,300	44,100	40,400	—	—
		1750	87,100	86,900	37,900	30,800	55	51
K	None	1500	79,600	87,300	33,500	38,800	—	—
		1750	83,400	84,700	34,800	35,300	63	62
K	Hot end	1500	79,500	81,000	31,100	43,200	—	—
		1750	83,700	86,200	30,400	26,100	53	55
K	Cold end	1500	86,700	82,300	39,300	45,500	—	—
		1750	85,700	77,000	37,100	42,300	76	58
None	None	1500	92,500	93,000	42,000	44,000	45	50
		1750	82,000	86,000	27,000	28,000	58	55
As-received material			94,000		37,000		70	

Table 9. Room temperature tensile test results, type 410 stainless steel

Liquid metal	Y location	Test at °F	Room temperature properties					
			Tensile strength		Yield strength		Elongation, %	
			Hot tab	Cold tab	Hot tab	Cold tab	Hot tab	Cold tab
Li	None	1500	67,200	Sd[a]	31,600	Sd	31	—
		1750	160,100	70,700	120,900	39,000	14	27
Li	Hot end	1500	67,000	73,200	37,500	41,400	33	36
		1750	157,600	74,300	123,100	33,500	14	24
Li	Cold end	1500	75,500	72,400	31,400	40,000	32	31
		1750	163,700	110,300	138,800	72,200	15	10
Cs	None	1500	73,000	74,100	45,500	36,800	36	32
		1750	130,200	114,000	93,900	45,200	16	19
Cs	Hot end	1500	66,300	74,200	35,100	44,800	37	36
		1750	123,000	68,600	78,800	37,700	15	37
Cs	Cold end	1500	72,100	75,400	30,800	30,700	33	35
		1750	155,400	67,100	119,500	36,600	10	37
Rb	None	1500	74,700	63,800	31,600	37,700	36	39
		1750	153,900	73,800	133,700	44,200	13	42
Rb	Hot end	1500	73,500	Sd	41,900	Sd	36	—
		1750	190,900	65,900	163,100	36,800	26	43
Rb	Cold end	1500	69,600	74,600	44,900	47,000	38	36
		1750	163,000	155,300	137,300	127,700	22	25
K	None	1500	75,100	65,500	29,100	46,200	35	41
		1750	136,900	158,500	114,400	133,700	16	8
K	Hot end	1500	89,400	72,400	40,400	42,900	26	35
		1750	153,600	67,000	104,200	39,000	12	44
K	Cold end	1500	89,400	71,500	51,800	40,900	27	35
		1750	159,200	67,700	128,700	43,700	57	45
None	None[b]	1500	184,000	155,000	147,000	120,000	15	13
		1750	178,000	162,000	131,000	127,000	17	11
As-received material			73,000		40,000		50	

[a]Sd = specimens damaged during testing.

[b]More rapid cooling rate of external specimens resulted in martinsitic transformation in 1500°F tests.
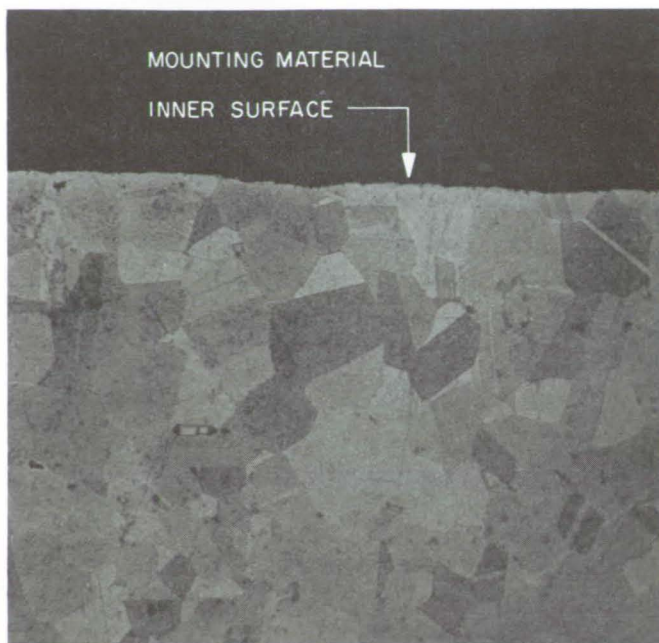
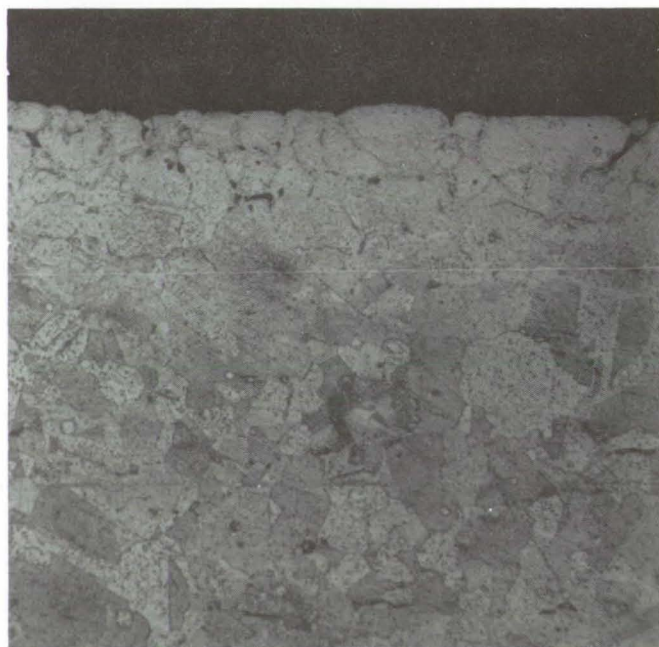**Fig. 5. Hot end of type 321 stainless steel-potassium capsule, ungettered, tested at 1500°F (250×)**

Fig. 6. Hot end of type 321 stainless steel-lithium capsule, ungettered, tested at 1500°F (250×)

Yttrium gettering resulted in severe dissimilar metal mass transfer and reaction (Figs. 7 and 8). The subsurface porosity that was produced in the ungettered capsule was not present in the gettered capsule containing lithium at 1500°F.

An increase in test temperature to 1750°F did not produce any observable change in microstructural appearance of the cesium or rubidium test capsules (Fig. 9).

a. Type 321 stainless steel data. The weight change data from the type 321 stainless steel-lithium capsule at 1750°F indicated a lack of lithium circulation. This indication is supported by metallographic observations, shown in Fig. 10. Little attack of the capsule was observed, although a precipitation layer apparently was produced during cooling of the test capsule. The gettered lithium capsules displayed an extensive reaction layer as a result of dissimilar metal mass transfer (Fig. 11).

Weight change data indicated slight temperature gradient mass transfer with potassium in the ungettered type 321 stainless steel capsule at 1750°F. A very thin deposit was observed on the cold end of the test capsule. No indication of preferential attack was present in this test capsule.

b. Type 410 stainless steel data. Metallographic examination of the type 410 stainless steel exposed to cesium, rubidium, or potassium displayed surface roughening, but no preferential grain boundary attack at either test temperature. Figure 12 is typical of these samples. The ungettered potassium capsule tested at 1750°F displayed a lack of attack of retained austenite (Fig. 13) as did the cesium test capsule (Fig. 14).

The mode of attack of the lithium varied with temperature. At 1750°F, the mode of attack was a general dissolution with slight indications of preferential solution of grain boundaries (Fig. 15). At this temperature, the type 410 stainless steel should be austenitic.

In the 1500°F range, the structure is mixed austenite, ferrite, and carbide. The mode of attack in this range is heavily intergranular (Fig. 16) and very prominent because of the large grain size. Further reduction of test temperature to 1200°F (the cold end of the 1500°F test) also produced intergranular penetration (Fig. 17).

4. Chemical analyses data. Analyses of the starting materials used are given in Table 2. Samples for analyses after test were taken from the tensile test tabs, using a full cross section; thus, the results indicate gross material variations. Microprobe analyses were used to obtain an indication of surface depletion effects.
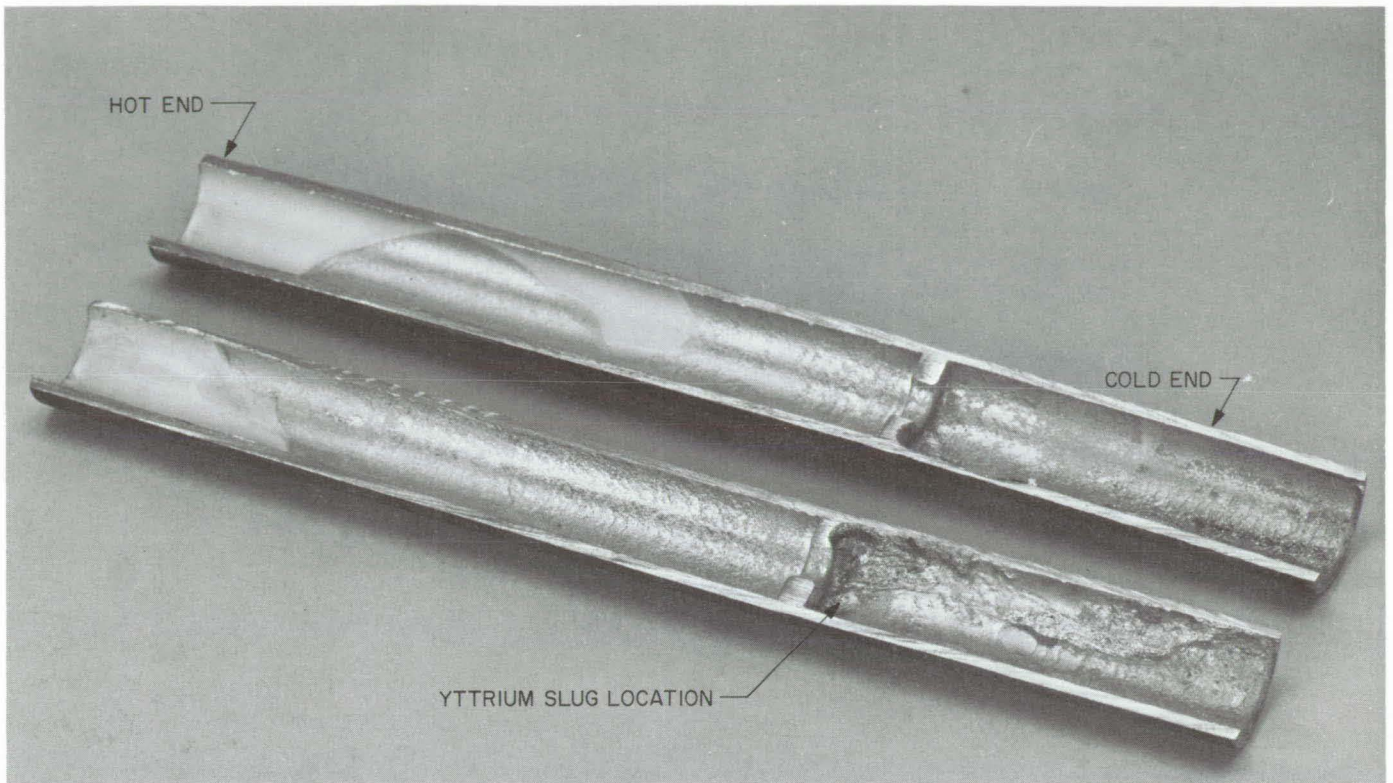
Fig. 7. Dissimilar metal mass transfer in type 321 stainless steel-lithium capsule, yttrium in cold end, tested at 1500°F

Fig. 8. Hot end of type 321 stainless steel-lithium capsule, yttrium in cold end, tested at 1500°F (250×)

Fig. 9. Hot end of type 321 stainless steel-rubidium capsule, ungettered, tested at 1750°F (250×)

Fig. 10. Hot end of type 321 stainless steel-lithium capsule, ungettered, tested at 1750°F (250×)

Fig. 12. Hot end of type 410 stainless steel-potassium capsule, ungettered, tested at 1500°F (250×)

Fig. 13. Cold end of type 410 stainless steel-potassium capsule, ungettered, tested at 1750°F (250×)

Fig. 11. Cold end of type 321 stainless steel-lithium capsule, yttrium in cold end, tested at 1750°F (250×)

Fig. 14. Cold end of type 410 stainless steel-cesium
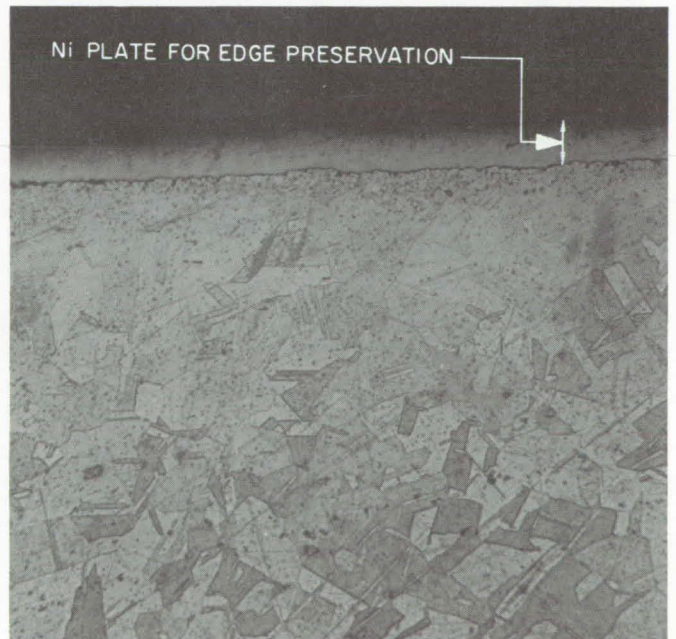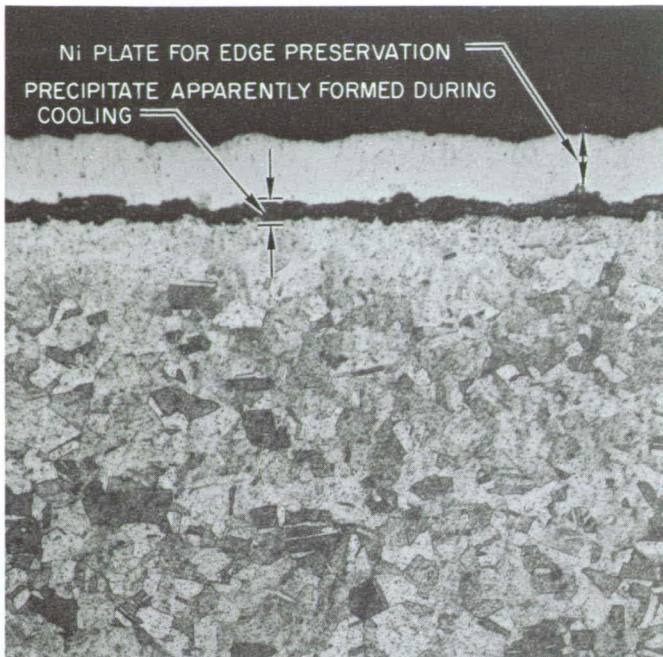capsule, ungettered, tested at 1750°F (250×)

Fig. 16. Cold end of type 410 stainless steel-lithium
capsule, ungettered, tested at 1750°F (250×)

Fig. 15. Hot end of type 410 stainless steel-lithium
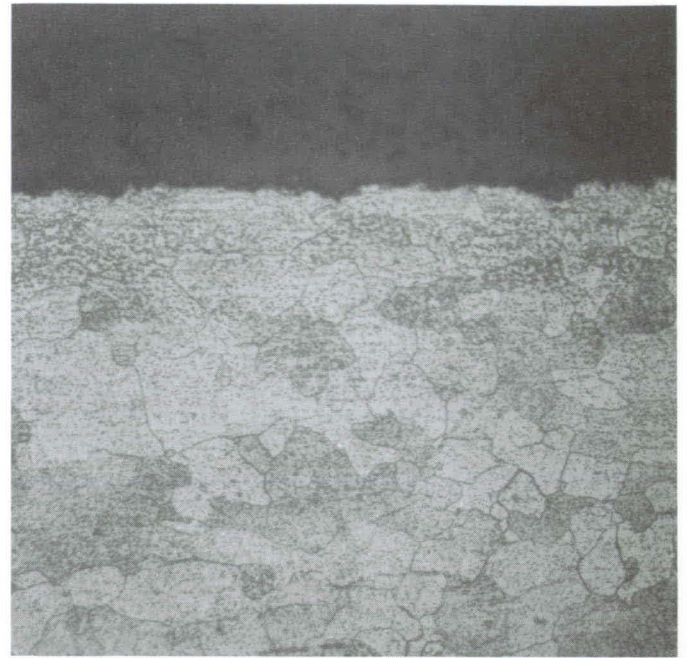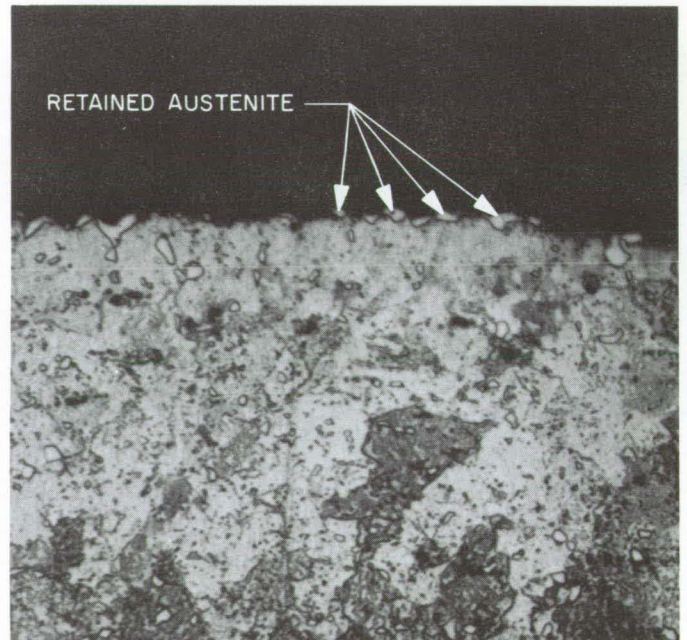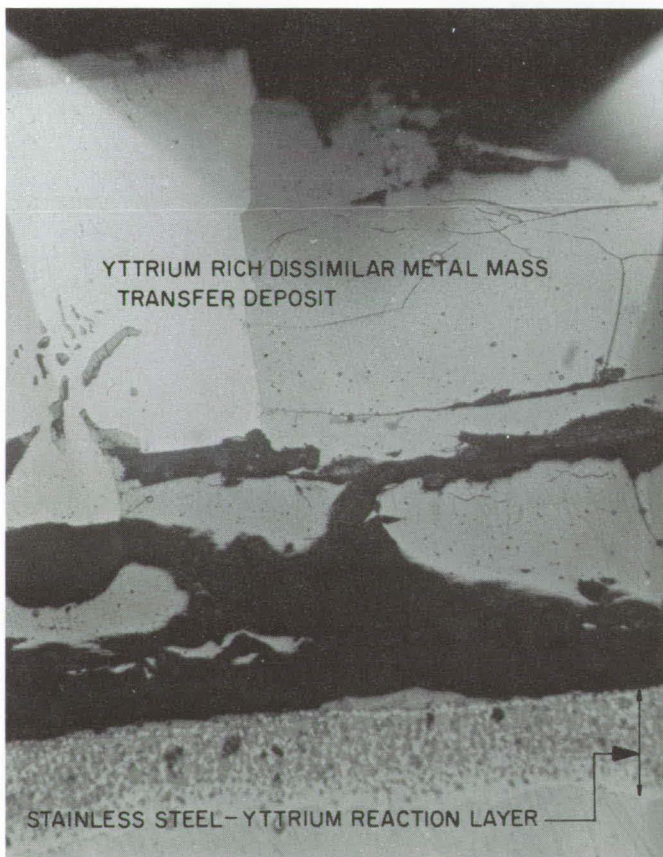capsule, ungettered, tested at 1750°F (250×)

Fig. 17. Cold end of type 410 stainless steel-lithium
capsule, ungettered, tested at 1500°F (250×)

The gross effects of potassium and lithium on type 321 stainless steel are given in Table 10. No change in gross chemistry of the material was detected after lithium exposure either with or without yttrium gettering; the high nickel content in the starting material was attributed to scatter in the analyses data, rather than a true effect.

Potassium exposure produced no change in the substitutional elements of the type 321 stainless steel; however, a buildup of oxygen content did occur in both the gettered and ungettered test capsules. The lack of effect of the yttrium gettering slug on oxygen buildup can probably be attributed to the small surface area of the yttrium

Table 10. Analyses of type 321 stainless steel after potassium and lithium exposure[a]

Element	Ungettered K capsule		Gettered K capsule[b]		Starting material	Ungettered Li capsule		Gettered Li capsule[b]	
	Cold end	Hot end	Cold end	Hot end		Cold end	Hot end	Cold end	Hot end
Cr	17.70	17.65	17.70	17.80	17.35	17.80	17.80	17.80	17.95
Mn	1.82	1.85	1.77	1.77	1.62	1.78	1.78	1.74	1.71
Ni	9.80	9.90	9.85	9.85	11.20	9.85	9.85	9.45	9.25
Si	0.68	0.69	0.66	0.69	0.72	0.69	0.69	0.64	0.67
Ti	0.51	0.50	0.50	0.51	0.47	0.50	0.51	0.44	0.44
C	0.07	0.07	0.04	0.07	0.08	0.05	0.07	0.06	0.06
H	6 ppm	1 ppm	3 ppm	3 ppm	1 ppm	1 ppm	8 ppm	3 ppm	2 ppm
N	0.009	0.011	0.010	0.008	0.010	0.013	0.010	0.012	0.011
O	0.022	0.009	0.043	0.022	0.006	0.007	0.008	0.007	0.010
P	0.025	0.026	0.027	0.028	0.018	0.020	0.025	0.022	0.019
S	0.008	0.007	0.008	0.008	0.005	0.006	0.008	0.007	0.007

[a]Conditions: 500 h, 1750°F maximum, and 300°F ΔT; measurements are in %, unless noted otherwise.
[b]Yttrium in cold end.

Table 11. Microprobe data from type 321 stainless steel

Liquid metal	Ungettered capsules		Yttrium gettered capsules	
	1500°F maximum, 300°F ΔT	1750°F maximum, 300°F ΔT	1500°F maximum, 300°F ΔT	1750°F maximum, 300°F ΔT
Li	No effects found	Hot end: 20% depleted in Ni, Cr, Cu, and Mn to 40μm Cold end: 50% enriched in Ni and Mn to 30μm	Hot end: 50% depleted in Ni, Cu, and Si and 25% enriched in Cr to 30μm Cold end: 20% depletion Cu to 30μm	Hot end: 75% depletion Ni to 175μm 25% enrichment Cr to 175μm 25% depletion Cu to 175μm 50% depletion Si to 175μm Cold end: 25% depletion Cu to 30μm 25% enrichment Mn to 30μm 50% enrichment Ti to 30μm 50% depletion Si to 30μm
Cs	No effects found	Not analyzed	No effects found	Not analyzed
Rb	Very slight, shallow, Cu depletion (~10%)	Not analyzed	Very slight, shallow, Cu depletion (~10%)	Not analyzed
K	Very slight, shallow, Cu depletion (~10%)	Not analyzed	Very slight, shallow, Cu depletion (~10%); 50% depletion of Ti to a depth of 25μm on hot end	Not analyzed

compared to the area of the test capsule, since the rate of oxygen uptake by a getter appears to be controlled by the diffusion rate of oxygen through the getter. Free-energy considerations would predict gettering of oxygen from potassium by the titanium addition in the type 321 stainless steel. This did not occur with the lithium, nor would it be predicted from free-energy considerations (Table 3).

Microprobe data for the type 321 stainless steel (Table 11) produced no indications of preferential surface depletion of alloying additions with cesium at 1500°F. Rubidium and potassium produced very slight, shallow leaching of copper from the type 321 stainless steel. Potassium, in addition to copper leaching, produced surface depletion of titanium from the hot end of the type 321 stainless steel test capsule.

In the ungettered lithium capsules of type 321 stainless steel, nickel and manganese appeared susceptible to temperature gradient mass transfer in that enrichment of these two metals occurred in the cold tabs. In addition, dissolution of chromium and copper occurred at the hot end of the capsule. Large increases in the degree of preferential attack occurred as a result of yttrium gettering in the lithium capsule.

Dissimilar metal mass transfer deposits from the type 321 stainless steel-lithium capsules tested at 1500°F were analyzed with the results as shown in Table 12. Deposits from the cold end of the capsule indicated a yttrium-chromium compound with little nickel and almost no iron present. Larger amounts of iron and nickel were present in the sample taken from the hot end of the capsule. Thus, based on solubility data of Ref. 10 (Fig. 2), the preferential removal of nickel was allowed by its high solubility in lithium where much of it presumably remained during the test. The chromium, because of its lower solubility, tended to diffuse inward rather than dissolving in the lithium producing enrichment at the inner surface. The chromium, which was dissolved, reacted with the yttrium to form a yttrium-chromium compound.

Analyses of the type 410 stainless steel after alkali metal exposure are given in Tables 13 and 14. The observed effects in this system were much less complex, since dissimilar metal mass transfer was essentially absent.

The only gross change in substitutional element composition appeared to be a temperature gradient mass

Table 12. Analyses of mass transfer deposits from 1500°F, type 321 stainless steel-lithium capsule with yttrium gettering at cold end

Element	Hot end of capsule, %	Cold end of capsule, %
Y	45.0	59.0
Fe	30.0	1.0
Ni	7.6	2.3
Cr	15.0	36.0
Si	0.70	0.23
Mn	0.81	0.30
Mg	0.10	0.13
Cu	0.15	0.092
Al	0.14	0.071
Mo	0.13	ND[a]
Sn	ND	ND
Ti	0.058	ND
Ca	0.12	0.11
B	0.045	0.061
Other	ND	ND

[a]ND = not detected.

transfer of nickel in the ungettered lithium capsule at 1750°F. This change was not confirmed by microprobe analyses, however.

Microprobe analyses indicated no effects with cesium, rubidium, or potassium in the gettered or ungettered condition. Lithium produced effects similar to those in the type 321 stainless steel, namely preferential solution of copper and silicon, some temperature gradient mass transfer nickel and manganese, and chromium enrichment in the hot tab of the ungettered capsule.

Movement of interstitial elements was much more extensive in the type 410 stainless steel, since gettering elements were present only as the yttrium slug.

Carbon transfer to the cold end of the capsule was considerable in the ungettered capsules of both lithium and potassium. Gettering with yttrium minimized this effect. Nitrogen content of the type 410 stainless steel

Table 13. Analyses of type 410 stainless steel after potassium and lithium exposure[a]

Element	Ungettered K capsule		Gettered K capsule[b]		Starting material	Ungettered Li capsule		Gettered Li capsulue[b]	
	Cold end	Hot end	Cold end	Hot end		Cold end	Hot end	Cold end	Hot end
Cr	12.85	12.60	12.80	12.65	12.00	12.40	12.75	12.60	12.50
Mn	0.35	0.34	0.36	0.30	0.29	0.36	0.37	0.33	0.30
Ni	0.31	0.31	0.31	0.32	0.31	0.40	0.28	0.32	0.32
Si	0.42	0.41	0.41	0.41	0.48	0.45	0.41	0.39	0.39
C	0.13	0.06	0.08	0.10	0.12	0.28	0.13	0.11	0.13
H	3 ppm	1 ppm	2 ppm	<1 ppm	5 ppm	10 ppm	2 ppm	5 ppm	5 ppm
N	0.006	0.007	0.002	0.007	0.030	0.016	0.008	0.009	0.005
O	0.013	0.010	0.010	0.016	0.012	0.033	0.007	0.021	0.012
P	0.015	0.015	0.015	0.015	0.018	0.014	0.015	0.013	0.010
S	0.027	0.010	0.007	0.006	0.010	0.016	0.015	0.013	0.010

[a]Conditions: 500 h, 1750°F maximum, and 300°F ΔT; measurements are in %, unless noted otherwise.
[b]Yttrium in cold end.

Table 14. Microprobe data from type 410 stainless steel

Liquid metal	Ungettered capsules		Yttrium gettered capsules	
	1500°F maximum, 300°F ΔT	1750°F maximum, 300°F ΔT	1500°F maximum, 300°F ΔT	1750°F maximum, 300°F ΔT
Li	Hot end: 10% depletion Cu to 50μm 40% depletion Si to 50μm Cold end: 40% depletion Si to 25μm 10% enrichment Mn to 25μm	Hot end: 40% depletion Si to >50μm 15% depletion Mn to 40μm 10% depletion Cu to >50μm 20% enrichment Cr to 30μm Cold end: 30% enrichment Mn to 10μm 60% depletion Si to >50μm	Hot end: 20% depletion of Si and Cu to > 50μm Cold end: 50% depletion Si to 25μm 20% enrichment Ni to < 10μm	Hot end: 40% depletion Si to 25μm Cold end: 10% enrichment Ni to 20μm 30% enrichment Mn to 25μm 40% depletion Cu to 20μm
Cs	No effects found	Not analyzed	No effects found	Not analyzed
Rb	No effects found	Not analyzed	No effects found	Not analyzed
K	No effects found	Not analyzed	No effects found	Not analyzed

was marked by a reduction in the gettered and ungettered capsules of both lithium and potassium.

5. Microhardness readings. The microhardness readings obtained on the type 321 stainless steel capsules were indicative of the thermal environment as well as corrosive effects. Readings obtained on the 1500°F ungettered potassium capsule indicated surface hardening at the cold end of the capsule. This indication coordinates with the chemical analyses results that indicate oxygen pickup. A similar increase was not observed in

the 1750°F test capsule despite chemical analyses indicating a similar oxygen buildup. This difference could be attributed to the variation of diffusion rate of oxygen with temperature, allowing a steeper concentration gradient to exist in the lower temperature capsule.

Considerable variation in microprobe hardness readings was obtained in the type 410 stainless steel samples due to the large variations in the amount of martensite present. No clear cut verification of chemical analysis effects were obtained during microhardness testing of these series of test capsules.

6. Summary of results. Negligible mass transfer was observed at either test temperature (1500 or 1750°F) with cesium, rubidium, and potassium in type 321 stainless steel. Lithium produced an order of magnitude more corrosion than the other three alkali metals in type 321 stainless steel.

Yttrium gettering had no effect on corrosion rates in type 321 stainless steel at 1500°F with cesium, rubidium, and potassium. Dissimilar metal mass transfer between the stainless steel and the yttrium occurred at 1500°F with lithium and at 1750°F with all four liquid metals.

No dissimilar metal mass transfer was observed between the yttrium and the type 410 stainless steel. Test tabs in the hot and cold ends of the type 410 stainless steel displayed weight losses at both test temperatures indicating predominance of dissolution corrosion rather than mass transfer. Weight changes were an order of magnitude greater with the type 410 stainless than with the type 321 stainless steel and increased another order of magnitude with increased test temperature. Type 321 stainless steel displayed little weight change with increased test temperature.

No room-temperature tensile test effects were observed which could be attributed to alkali metal corrosion.

Increases in oxygen content of the type 321 stainless steel were observed in the potassium tests, but not in the lithium tests. Lithium did produce a preferential leaching of copper, manganese, nickel, and silicon from both stainless steels.

Carbon transfer from the hot end to the cold end of the type 410 stainless steel was observed with both potassium and lithium. Yttrium gettering essentially eliminated this effect. Reduction of nitrogen content occurred in the type 410 stainless steel under all conditions.

IV. Discussion and Conclusions

The data gathered indicate that type 321 stainless steel is suitable for containment of cesium or rubidium at temperatures up to the limit of structural capability. Potassium was shown to be somewhat more aggressive than cesium or rubidium. The titanium stabilization of type 321 stainless steel appears to have eliminated the carbon transfer problem encountered in experiments at Oak Ridge with type 316 stainless steel. However, oxygen transfer was still observed. The weight changes encountered in

the tilting capsules at 1750°F were comparable to the weight changes observed in forced convection loops at 1600°F by workers at Oak Ridge. Although the effect of flow rate was not evaluated and the increased flow rates in pumped systems may adversely affect the corrosion resistance of the stainless steel, the almost total lack of mass transfer and solution attack in these tests would make the stabilized type 321 stainless steel alloy appear promising for application under forced flow conditions.

Thus, the presence of a gettering agent in the alloy has eliminated the carbon transfer problem which has an adverse effect on mechanical properties, but general solution and mass transfer have shown little change. The conclusion presented by workers at Oak Ridge, that the corrosion of a conventional iron or cobalt-base alloy appears to be from the formation of mass transfer crystals rather than from dissolutive attack, also appears valid for the type 321 stabilized stainless steel.

In unstabilized stainless steel, the possibility of reducing the extent of carbon transfer appears to exist via the use of flow stream gettering agents. This conclusion is based on the data gathered in type 410 stainless steel tests where yttrium present in the flow stream considerably reduced the transfer of carbon in capsules containing lithium or potassium.

Analyses for nitrogen transfer are in agreement with data gathered by R. W. Harrison (Ref. 24) showing that stabilization of stainless steel eliminated nitrogen transfer to gettering elements in dissimilar metals present in the flow stream. Reduction of nitrogen content did occur in all portions of the unstabilized alloy test capsule.

The lithium produced a subsurface porosity in the stabilized type 321 stainless steel; this porosity appeared to be eliminated by the addition of yttrium to the flow stream. It is possible that the dissimilar metal mass-transfer layer produced this protection. However, the possibility of this technique reducing corrosion appears sufficiently promising that further investigation with other gettering metals less susceptible to dissimilar metal mass transfer is indicated.

Weight change data for the type 321 stainless steel follow the trend observed at Oak Ridge for pumped potassium loops of Haynes-25 in that little increase in corrosion rate was observed with an increase in operating temperature. Verification of this conclusion under forced circulation conditions has yet to be demonstrated.

Preferential leaching of alloying elements by all four liquid metals was very similar to that observed in Soviet studies on sodium (Ref. 27). They found that manganese, silicon, and nitrogen are undesirable constituents. Chemical analysis and microprobe data gathered in this study verified the preferential transfer of these elements as well as the traces of copper present in stainless steel.

The Soviet studies also concluded that alloys should have no more nickel than is needed to ensure structural stability, strength, and ductibility. The data gathered in this study tend to support this conclusion in the case of lithium, which produced preferential transfer of nickel, but with the provision that the amount of nickel present should be enough to produce an austenitic structure. No preferential transfer of nickel was observed with cesium, rubidium, or potassium, thus the conclusion does not appear valid for these alkali metals at the 8%-nickel level. This study is consistent with the Soviet conclusion that alloys should be stabilized.

References

1. Hoffman, E. E., *Corrosion of Materials by Lithium at Elevated Temperatures*, Report ORNL-2924. Oak Ridge National Laboratory, Tenn., Oct. 27, 1960.

2. Jansen, D. H., and Hoffman, E. E., *Type 316 Stainless Steel, Inconel and Haynes Alloy No. 25 Natural Circulation Boiling — Potassium Corrosion Test Loops*, Report ORNL-3790. Oak Ridge National Laboratory, Tenn., June 1965.

3. Young, P. F., *Design and Operation of 1800°F Pumped Boiling Rubidium Loop System and Determination of Density and Vapor Pressure of Rubidium Between 174 and 1800°F*, Report NGN 8034. Aerojet-General Nucleonics, San Ramon, Calif., May 1961.

4. Glassman, A. J., and Futral, S. M., *Analytical Study of Turbine-Geometry Characteristics for Alkali-Metal Turboelectric Space Power Systems*, NASA TN O-1710. National Aeronautics and Space Administration, Washington, D. C., May 1963.

5. Frye, J. H., Jr., et al., *Metals and Ceramics Division Annual Report Ending June 30, 1964*, Report ORNL-3670. Oak Ridge National Laboratory, Tenn., Oct. 1964.

6. McKisson, R. L., and Eichelberger, R. L., "Solubility and Diffusion Studies of Ultra Pure Transition Elements in Ultra Pure Alkali Metals," Atomics International Summary presented at the AEC-NASA Liquid Metals Information Meeting, Gatlinburg, Tenn., Apr. 21–23, 1965.

7. Swisher, J. H., *Solubility of Iron, Nickel, and Cobalt in Liquid Potassium and Effect of Oxygen Gettering Agents on Iron Solubility*, NASA TN D-2734. Lewis Research Center, Cleveland, Ohio, Mar. 1965.

8. Freed, M. S., and Kelly, K. J., *Corrosion of Columbium Base and Other Structural Alloys in High-Temperature Lithium*, Report PWAC-355. Pratt and Whitney Aircraft Canel Div. of United Aircraft Corp., Middletown, Conn., June 30, 1961.

9. Ault, G. M., *A Decade of Progress in Refractory Metals*, NASA TM X-52135. National Aeronautics and Space Administration, Washington, D. C., June 1965.

References (contd)

10. DeStefano, J. R., *Corrosion of Refractory Metals by Lithium*, Report ORNL-3551. Oak Ridge National Laboratory, Tenn., Mar. 1964.

11. Ginell, W. S., and Teitel, R. J., "Solubility of Transition Metals in Molten Potassium," Douglas Aircraft Co. paper presented at the AEC-NASA Liquid Metals Information Meeting, Gatlinburg, Tenn., Apr. 21–23, 1965.

12. Ginell, W. S., and Teitel, R. J., "Determination of Solubility of Several Transition Metals in Molten Potassium," *Trans. Am. Nucl. Soc.*, Vol. 8, No. 2, pp. 393–394, Nov. 1965. .

13. Wenslow, P. M., "Synopsis of Cesium Compatibility," paper presented at the AEC-NASA Liquid Metals Information Meeting, Gatlinburg, Tenn., Apr. 21–23, 1965.

14. Chandler, W. T., and Hoffman, N. J., *Effects of Liquid and Vapor Cesium on Container Metals*, Report ASD-TDR-62-965. Rocketdyne Div., North American Aviation, Inc., Canoga Park, Calif., Mar. 1963.

15. Hall, W. B., and Kessler, S. W., *Cesium Compatibility of Thermionic Converter Structural Materials*, Report AD-463878. Electronic Component and Devices Div., Radio Corp. of America, Lancaster, Pa., 1964.

16. Tepper, F., and Greer, J., *Factors Affecting the Compatibility of Liquid Cesium with Containment Metals*, Report ASD-TDR-63-824 (prepared for Air Force Materials Laboratory). Mine Safety Appliances Research Corp., Callery, Pa., Sept. 1963.

17. Tepper, F., and Greer, J., *Factors Affecting Compatibility of Liquid Cesium with Containment Materials*, Report AFML-TR-64-327. Mine Safety Appliances Research Corp., Callery, Pa., Nov. 1964.

18. Young, P. F., et al., *Determination of Temperature Coefficient of Solubility of Various Metals in Rubidium and the Corrosive Effects of Rubidium on Various Alloys at Temperatures from 1000° to 2000°F*, USAEC Report AGN-8063. Aerojet-General Nucleonics, San Ramon, Calif., July 1962.

19. Nevsorev, B. A., "The Nature of Oxygen in Liquid Sodium," in *Proceedings of the IAEA Conference on Corrosion of Reactor Materials, Europahaus, Salsburg, Austria, June 4–8, 1962*. Vol. II, p. 279, International Atomic Energy Agency, Vienna, Austria, 1962.

20. Cleary, R. E., et al., "Solubility Studies in Alkali Metals," USAEC Report CNLM-6335. Pratt and Whitney Aircraft Canel Div. of United Aircraft Corp., Middletown, Conn., Apr. 21, 1965.

21. Litman, A. P., *The Effect of Oxygen on the Corrosion of Niobium by Liquid Potassium*, Report ORNL 3751. Oak Ridge National Laboratory, Tenn., July 1965.

22. Stang, J. H., "Corrosion by Liquid Metals," *Reactor Mater.*, Vol. 8, No. 2, p. 90, 1965.

References (contd)

23. Goldmann, K., Hyman, N., Kostman, S., and McKee, J., "Carbon and Nitrogen Transfer in a Type 316 Stainless Steel, Cb-1Zr Liquid Potassium System," *Nucl. Appl.*, Vol. 3, No. 2, pp. 117–126, Feb. 1967.

24. Harrison, R. W., "Alkali-Metal Corrosion Studies on Materials for Advanced Space Power Systems," *Trans. Am. Nucl. Soc.*, Vol. 8, No. 2, pp. 392–393, Nov. 1965.

25. Weeks, J. R., Klamut, C. J., and Gurinsky, D. H., "Corrosion by the Alkali Metals," in *Alkali Metal Coolants*, proceedings of the Symposium on Alkali Metal Coolants—Corrosion Studies and System Operating Experience, held in Vienna, Nov. 28—Dec. 2, 1966. International Atomic Energy Agency, Vienna, 1967.

26. Brewer, L., et al., "Thermodynamic and Physical Properties of Nitrides, Carbides, Sulfides, Silicides, and Phosphides," Paper 4 of *The Chemistry and Metallurgy of Miscellaneous Materials,* pp. 40–59. Edited by L. L. Quill. McGraw-Hill Book Co., Inc., New York, 1950.

27. Agapova, N. P., Ioltukhovskiy, A. G., and Romaneev, V. V., "Behavior of Stainless Steel in Sodium in the 600–900°C Temperature Range," Paper SM-85/51, presented at the International Atomic Energy Agency Symposium on Alkali Metal Coolants-Corrosion Studies and System Operating Experience, Vienna, Austria, Nov. 28–Dec. 2, 1966.